IJL, Issue 2, Vol. 23, 2024
https://doi.org/10.31900/ijl.v23i2.478

Research Article

Evaluation of Anti-Cancer Activity of Silver@Gold Nanoparticles by Hybrid Technique

Zainab Shaheed Kadhim, Haider Y. Hammod*

Department of Physics, College of Science for Women, University of Baghdad, Iraq
** Email address of the Corresponding Author:dr.hayder.y.phy@gmail.com*

Article history: Received 23 May 2024; Revised 20 Jul. 2024; Accepted 1 Aug. 2024; Published online 15 Dec. 2024

Abstract: This research deals with the evaluation of the anti-cancer activity of Ag@Au NPs synthesis by a hybrid system combining laser and plasma jet techniques. The effect of NPs on inhibiting the growth of breast cancer cells and normal cell lines was studied. Firstly, silver nanoparticles were prepared using a Nd:YAG laser with a wavelength of 1064 nm, a frequency of 6 Hz, an energy of 1000 mJ, and a number of pulses of 558. In the second step, we take different ratios between Ag NPs and gold salts as follows: (1:9, 2:8, and 3:7), respectively, and exposed to a plasma jet system for 3 minutes. The NPs were checked using X-ray diffraction, UV-vis spectroscopy, and field emission scanning electron microscopy (FE-SEM). The highest rate of inhibition of breast cancer cells was 66% after 48 hours when the concentration was 100% with a ratio of 3:7. As for its toxicity to normal cells, the highest toxicity was 16% after 24 hours when the concentration was 100% for 3:7. The expected results could provide new light on the effectiveness of these particles in treating cancer and stimulate future research in this field.

Keywords: Hybrid system, laser ablation, plasma jet, anticancer.

1. Introduction

Nanotechnology is the study and application of materials with sizes as small as 100 nanometers (nm). They are employed in a wide range of industries, including agriculture, food processing, material science, cosmetics, medicine, and diagnostics. Nano-sized inorganic compounds have demonstrated remarkable antibacterial activity at extremely low concentrations because of their high surface area-to-volume ratio and distinctive physical and chemical properties [1]. There are three primary methods available for producing nanoparticles: chemical, physical, and biological approaches [2].

Noble metal nanoparticles, such as gold and silver, are highly sought after due to their distinct optical, chemical, physical, and electrical properties. Au and Ag nanoparticles both demonstrate a plasmonic effect due to the scattering and absorption of light. Au nanoparticles (NPs) and Ag nanoparticles (NPs) exhibit insensitivity to physical variables such as light, air, electrical characteristics associated with size, magnetic properties, exceptional conductivity, and chemical stability [3].

The production of metal oxide and metal nanoparticles can be achieved by a straightforward method called Pulsed Laser Ablation in liquid environments (PLAL).The laser ablation process is significantly influenced by the specific properties of the laser beam employed, such as the number of pulses, wavelength, pulse duration, and energy. The ablation rate is directly proportional to the number of laser pulses, which is particularly evident in the case of dielectrics, semiconductors, and single metals [4]. PLAL offers a multitude of desirable advantages. This methodology is a direct and effective method for generating a large number of nanoparticles that are evenly dispersed in a liquid medium [5].

Plasma, often known as the fourth state of matter, is a plasma consisting of charged and neutral particles that interact together. Plasma encompasses gaseous nebulae, the interiors of stars, atmospheres, and interstellar hydrogen. Plasma consists of negatively charged electrons and positively charged ions of atoms, and it constitutes approximately 99% of all matter in the universe [6]. Plasma is often a gas that has been ionized. The process involves the aggregation of charged particles, including electrons, ions, and molecules. The term "ionized" refers to the presence of one or more free electrons [7].

Cancer encompasses a wide range of diseases, including liver, stomach, lung, bladder, colon, and breast cancers, which are the most prevalent. Given its prevalence among women, this study specifically targets breast cancer as opposed to other types of cancer. The expansion of breast cancer involves the activation or inactivation of several gene types that are necessary for promoting malignancy. While breast cancer is mainly a genetic disease affecting somatic cells, there are instances where it is associated with genetic disorders. Breast cancer is categorized as a metastatic neoplasm. It usually manifests in the axillary lymph nodes, but it can also metastasize to any location in the skeletal system or bone marrow [8].

In this study, the aim was to prepare Ag@Au nanoparticles using a hybrid system (laser-plasma jet) and test their inhibition on breast cancer and normal cells.

2. Experimental Procedures

2.1 synthesis of nanoparticles

2.1.1 Prepared Ag NPs using Nd:YAG system as a core

Using the pulsed laser ablation technique, Ag NPs were created in liquid (PLAL) and a pure silver plate (0.5×0.5) cm with a purity of 99.99%. They were then 5 ml of deionized water put in a 10–20 ml glass beaker and 5 cm away from the laser source. The laser source was a Q-switched Nd:YAG laser with a frequency of 6 Hz, wavelength of 1064 nm, and energy of 1000 mJ. As seen in Fig.1 (A).

(A) **(B)**

Fig.1. The prepared Ag@Au NPs by a hybrid system (A) Nd:YAG laser (B) plasma jet.

2.1.2 Prepared Au NPs using plasma jet as a shell

The (AuCl4•3H2O) hydrogen tetrachloroaurate trihydrate, which has a partial weight of 393.83 g/mol, a purity of ≥ 99.9%, and a concentration of 0.5 mM, has been prepared as a shell. The required weight is calculated using the following equation (1) [9]:

$$Concentration\left(\frac{mol}{liter}\right) = \frac{mass(g)}{Molecular\ weight\ \left(\frac{g}{mol}\right) * Volume\ (liter)} \qquad (1)$$

2.1.3 Prepared Ag@Au NPs

A cylindrical metal tube with a diameter of 1 mm is securely fastened in a vertical position by the catcher. With the plasma jet technique, the length of the plasma between the two electrodes was 1 cm, the flow meter was 3 liters/minute, the voltage was 20 kV, and the gas used was argon.
After that, we added Ag NPs prepared by the Nd:YAG method, as shown in Fig.2(a) to gold salts in the following ratios: (1:9, 2:8, and 3:7), respectively. The mixture was then exposed to the plasma system for 3 minutes until the color of the solution turned violet.

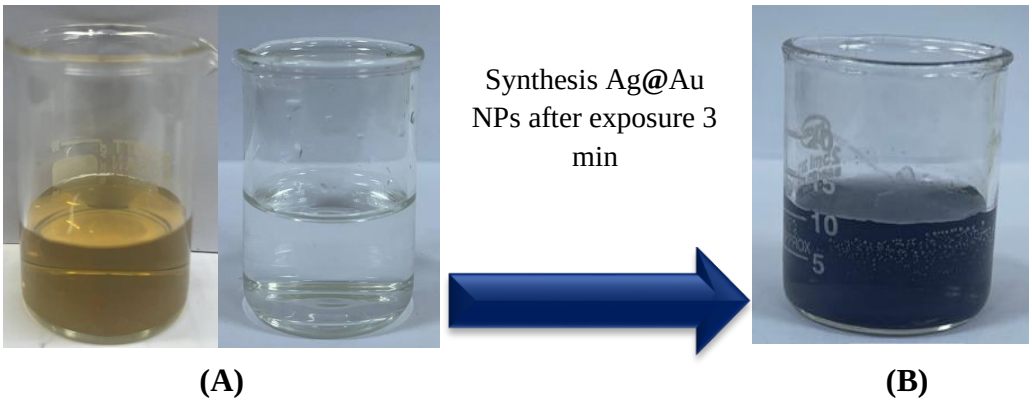

Fig.2. Preparation Ag@Au NPs (A) Ag NPs by Nd:YAG and gold salts (B) Ag@Au NPs by plasma jet.

2.2 The impact of prepared nanoparticles on breast cancer cells

This study utilized cell lines derived from cancer patients. The research utilized 96 (12×8) microtiter plates for tissue culture, with each plate being seeded with 10,000 cells. The cells were subsequently incubated at a temperature of 37 °C for a duration of 24 hours to form a monolayer, as confirmed by the use of an inverted microscope. In addition, a solution containing diluted silver nanoparticles (Ag NPs) and gold nanoparticles (Au NPs) is administered to the cells, whereas no treatment is given to the control wells. The indicated stages have been performed three times, following which they were subjected to re-incubation at a temperature of 37 °C. The growth medium was poured out after 48 hours of incubation. The methods were repeated three times to verify the authenticity, employing a 50µl crystal violet assay, followed by an incubation period of 20 minutes. The cells were observed using an inverted microscope, captured with a digital camera, and recorded individually to obtain the data. The results of the experiment are analyzed using Graph Pad Prism version 8 [9].

3. Results and Discussion

The reaction process causes the solutions' hue to change, which is connected to the creation of metal nanoparticles (NPs) made using the Ar jet technique and the metal salts' prepared solutions. The color shift gives the first hint regarding the formation of NPs during mixing in metal salt solutions. Metal particles take on their non-metal color due to surface plasmon resonance (SPR), which happens when a metal's particle diameter becomes close to a nanometer, as in the case of gold and silver. Thus, the spectrum analysis equipment has been applied at visible light wavelengths to prove the NPs formation. The ultraviolet-visible absorption spectra connected to colloidal Ag@Au NPs at different ratios (1:9, 2:8, and 3:7), and compare results (Ag NPs) only and at visible light wavelengths (590, 598,608) nm, respectively. In the ultraviolet-visible spectrum of Ag NPs when exposed to Nd:YAG laser, the sharp peak is at about 415 nm. As a varied Ag@Au NPs ratio, the UV-visible absorption spectra of colloidal Ag@Au NPs are shown in Figure 3.

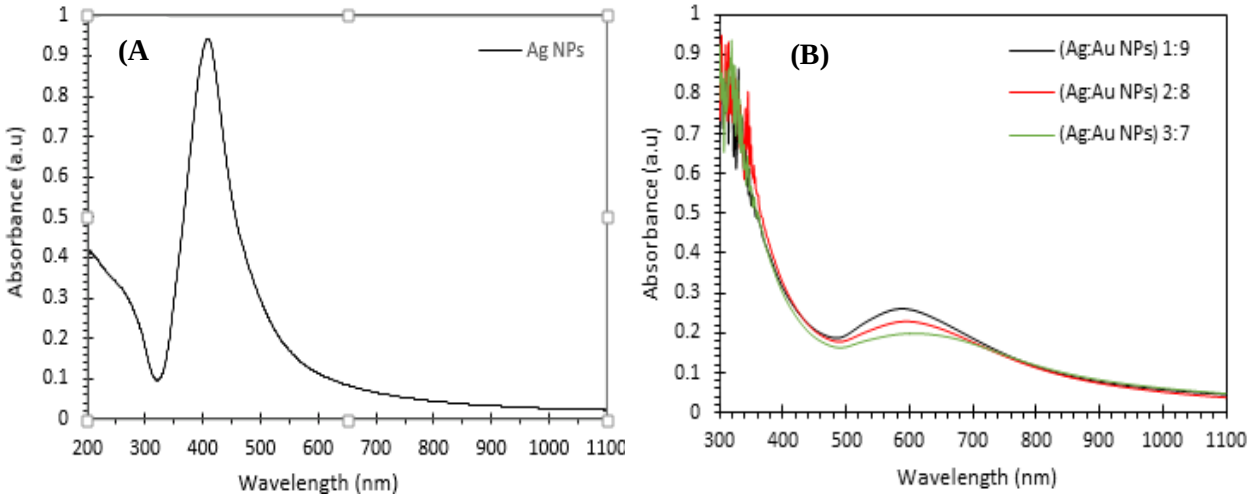

Fig. 3. UV-visible absorption spectrum of NPs prepared using hybrid (laser-plasma) system as a different ratios functions: (A) Ag NPs (B) Ag@Au NPs.

3.1 X-Ray Diffraction (XRD)

The dried Ag NPs produced by the pulse laser system were placed on a hot plate at 30°C. Figure.4 (A) shows the XRD Ag NPs spectrum, the peaks at angles of (38.29, 44.44, 64.56, and 77.64) correspond to (111), (200), (220), and (311) planes of Ag. The XRD analysis of Ag@Au NPs using a plasma jet revealed several Bragg reflection peaks at specific 2-theta values (38.12°, 44.3°, 46.21°, 54.83°, 64.42°, and 77.45°). These peaks correspond to the (111), (200), (231), (142), (220), and (311) planes of pure silver, as determined by the face-centered cubic structure, as shown in the Figure.4 (B). The aforementioned pattern has demonstrated that peaks' diffraction patterns cannot be replicated in other kinds of material, proving the prepared sample's purity and lack of additional impurities [10]. The crystal size of silver nanoparticles is 45 nm, and the crystal sizes of Ag@Au NPs for the following ratios (1:9, 2:8, 3:7) are (45, 48, and 17) nm, respectively, using the Debye-Scherer equation (2) [11].

$$D = \frac{k\lambda}{\beta \cos\theta} \qquad (2)$$

Where D is the crystallite size, k is the Scherer's constant (k = 0.9), λ for X-ray wavelength, and β for full width at half maximum (FWHM) of the peaks at the θ diffracting angle relative to Bragg's angle position.

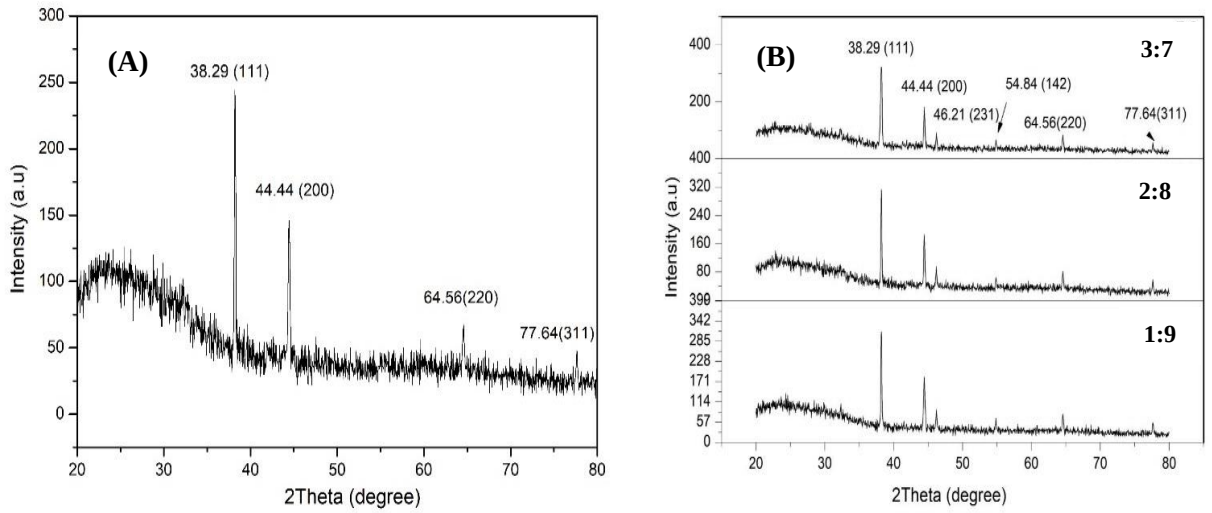

Fig.4. X-ray patterns of NPs prepared using a hybrid (laser-plasma) system as different ratios functions: (A) Ag NPs (B) Ag@Au NPs.

3.2 Field Emission Scanning Electron Microscopy Study (FE-SEM)

FE-SEM images show the morphological properties of Ag NPs and Ag@Au NPs synthesized with a plasma jet (see Figure 5).

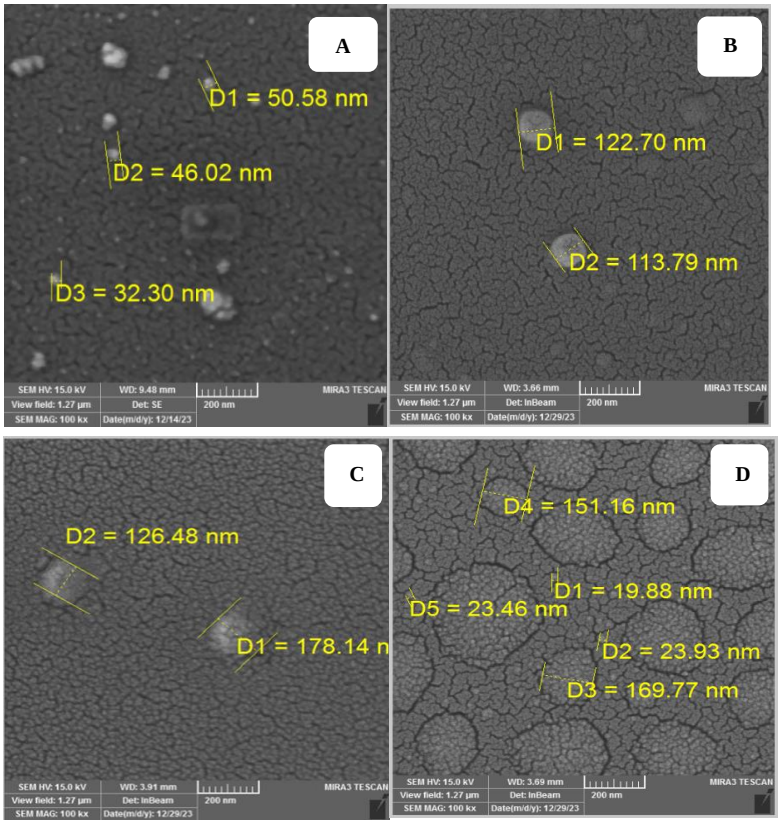

Fig.5. FE-SEM pictures of the colloidal nanoparticles: (A) Ag NPs (B) Ag@Au NPs 1:9 (C) Ag@Au NPs 2:8 (D) Ag@Au NPs 3:7.

Figure 5 (a) displays a well-dispersed picture of Ag NPs with a spherical shape and sizes ranging from 32 to 50 nm. The images revealed highly agglomerated spherical Ag@Au NPs in the sample, as determined by FESEM. It is likely that chemical processes or pre-experimental conditions led the spherical particles to cluster together and form agglomerated formations. This can occur due to forces between particles such as superposition and surface cross-linking. Agglomerated nanoparticles provided a significant benefit in preparation since they could influence the physical and chemical properties of the particles. It may result in an increase in particle interface area, leading to better surface interactions and performance.

3.3Transmission Electron Microscopy (TEM)

The synthesis of core/shell nanoparticles was confirmed using transmission electron microscopy (TEM) analysis utilizing the hybrid method was employed because of its capability to accurately determine the thickness and distance between the core and shells. TEM analysis provided further data regarding the morphology, dimensions, and clustering of the particles. The transmission electron microscopy (TEM) images reveal that the Ag@Au NPs exhibit a configuration of interlocking spheres, forming dense clusters. It is noteworthy that not all ratios demonstrate the synthesis of core/shell structures, particularly the 1:9 ratio. The reason for this is that the proportion of silver particles is significantly smaller than that of gold particles. Additionally, gold ions have the ability to reduce silver on their surface due to the electrical disparity. This prevents the formation of a silver core that is coated with a layer of gold, as depicted in Figure 6.

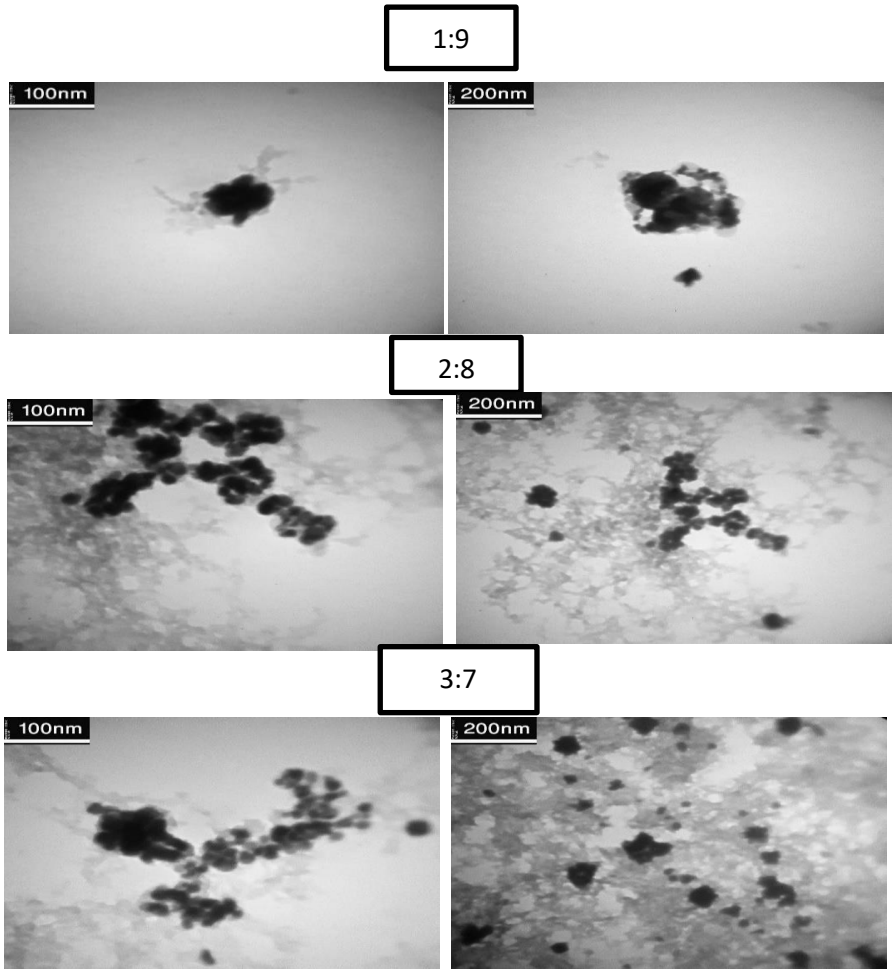

Fig.6. TEM image of Ag@Au NPs by the hybrid system.

Furthermore, TEM examination revealed the presence of two distinct zones. The core is represented by the dark inner area, while the light part around the dark region represents the shell. This confirms the synthesis of core/shell nanoparticles at the ratios of 2:8 and 3:7.

3.4 Cytotoxicity Assay

The cytotoxicity of the various series with Ag@Au NPs at different ratios has been evaluated in vitro using the normal cell line (REF) and the breast cancer cell line (MDA) after exposure for 24 and 48 hours. As shown in Fig.6 (A) and (B), respectively, the greatest rate of destruction for the breast cancer cell line (MDA) was 55% after 24 hours when the concentration of core-shell nanoparticles was 100% for 3:7 , and the greatest rate was 63% after 48 hours for 3:7. According to Fig.7 (A) and (B), for the normal cell line (REF), the highest toxicity was 16% after 24 hours when the concentration of core-shell nanoparticles was 100% for 3:7, and the lowest toxicity was 5.6% when the concentration was 12.5% for 1:9. Similarly, for the 48-hour period, the highest toxicity was 21% when the concentration was 100% for 2:8 and 3:7, and the lowest toxicity was 7% when the concentration was 12.5% for 1:9, which stars means [(*) refer ($p \leq 0.05$), (**) refer ($p \leq 0.01$), (***) refer ($p \leq 0.001$), and (****) refer ($p \leq 0.0001$)].

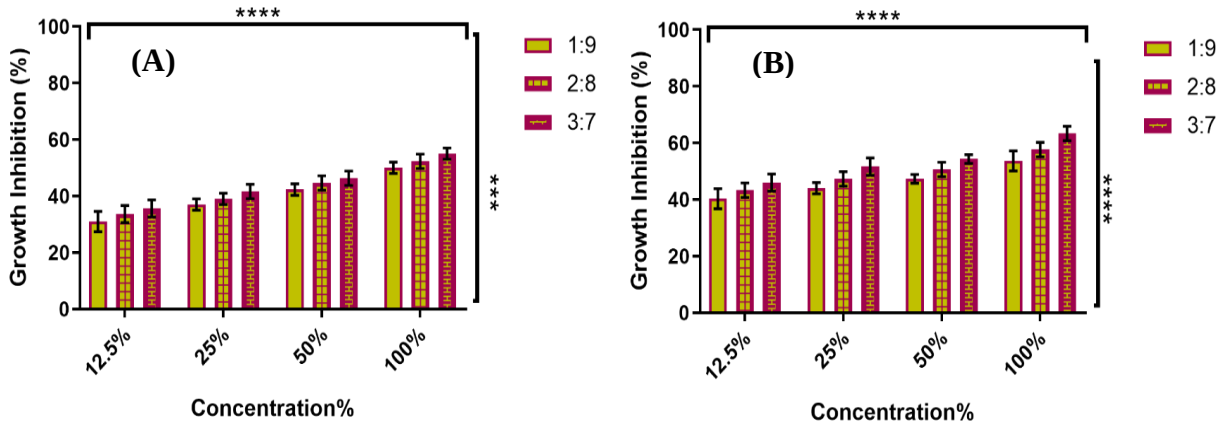

Fig.6. Growth inhibition of the breast cancer cells line (MDA) as different ratios of Ag@Au NPs: (A) After 24 hours (B) After 48 hours.

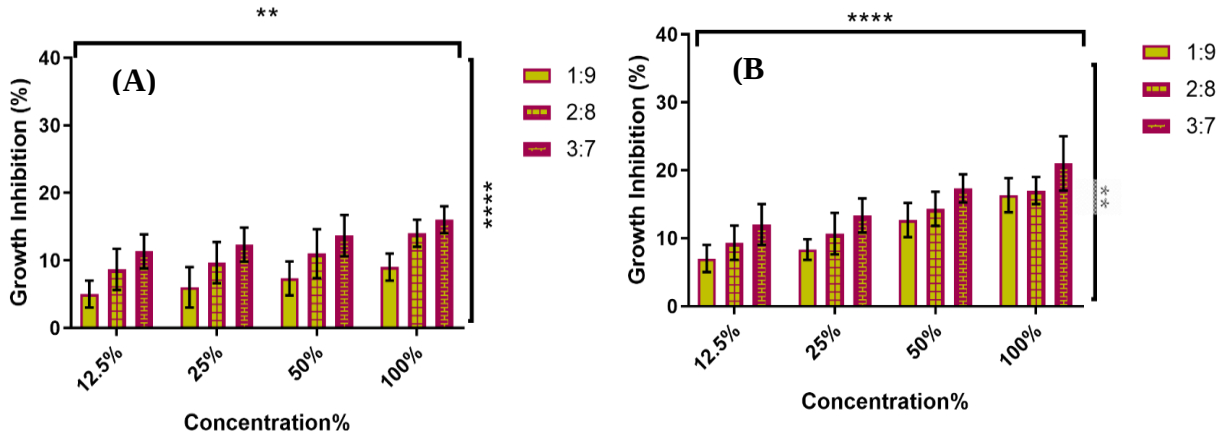

Fig.7. Growth inhibition of the normal cells line (REF) as different ratios of Ag@Au NPs: (A) After 24 hours (B) After 48 hours.

3. Conclusions

In conclusion, this research successfully evaluated the anti-cancer activity of gold-coated silver particles prepared using a hybrid system combining laser and plasma techniques. The study showed the ability of these particles to inhibit the growth of breast cancer cells, with the highest inhibition rate at 66% after 48 hours at a 100% concentration of 3:7. In addition, the toxicity was relatively low to normal cells, with the highest toxicity rate of 16% after 24 hours at 100% concentration for the same ratio. These results highlight the effectiveness of Ag@Au NPs in cancer treatment and pave the way for future research in this promising field.

References

[1] Shanan, Z. J., Abdalameer, N. K., & Ali, H. M. (2022). Zinc Oxide Nanoparticle Properties and Antimicrobial Activity. *International Journal of Nanoscience*, *21*(03), 2250017.
[2] Ijaz, I., Gilani, E., Nazir, A., & Bukhari, A. (2020). Detail review on chemical, physical and green synthesis, classification, characterizations and applications of nanoparticles. *Green Chemistry Letters and Reviews*, *13*(3), 223-245.
[3] Kamil, A. A., Bakr, N. A., Mubarak, T. H., & Al-Zanganawee, J. (2021). Synthesis and study of the optical and structural properties of Au and Ag nanoparticles by pulsed laser ablation (PLAL) technique. *Digest Journal of Nanomaterials & Biostructures (DJNB)*, *16*(4).
[4] Majeed, M. S., Mahmoud, S. M. M., Rasheed, R. M., & Rashad, A. A. (2024). Synthesis AgO Nanoparticles by Nd: Yag Laser with Different Pulse Energies. *Baghdad Science Journal*, *21*(1), 0217-0217.
[5] Nasif, H. K., Ahmed, B. M., & Aadim, K. A. (2021). Synthesis Emission Spectra of (LIPS) Technique for Cu, Ag Nanoparticles and their Antibacterial Activity. *Al-Mustansiriyah Journal of Science*, *32*(3), 49-57.
[6] Adil, B. H., Al-Shammari, A. M., & Murbat, H. H. (2020). Breast cancer treatment using cold atmospheric plasma generated by the FE-DBD scheme. *Clinical Plasma Medicine*, *19*, 100103.
[7] Mazhir, S. N., Abdullah, N. A., al-Ahmed, H. I., Harb, N. H., & Abdalameer, N. K. (2018). The effect of gas flow on plasma parameters induced by microwave. *Baghdad Science Journal*, *15*(2), 0205-0205.
[8] Ingvarsson, S. (2001, October). Breast cancer: introduction. In *seminars in CANCER BIOLOGY* (Vol. 11, No. 5, pp. 323-326). Academic Press.
[9] Mohammed, M. S., Adil, B. H., Obaid, A. S., & Al-Shammari, A. M. (2022, February). Plasma Jet Prepared Gold and Silver Nanoparticles to Induce Caspase-Independent Apoptosis in Digestive System Cancers. In Materials Science Forum (Vol. 1050, pp. 51-63). Trans Tech Publications Ltd.
[10] Abdullah, Q. N., Obaid, A. S., & Bououdina, M. (2018). Influence of gas carrier on morphological and optical properties of nanostructured In2O3 grown by solid-vapour process. Ceramics International, 44(5), 4699-4703.
[11] Kanagaraj, J., Senthilvelan, T., Panda, R. C., Aravindhan, R., & Mandal, A. B. (2014). Biosorption of trivalent chromium from wastewater: an approach towards Green chemistry. *Chemical Engineering & Technology*, *37*(10), 1741-1750.

تقييم النشاط المضاد للسرطان للجسيمات النانوية الفضة/الذهب بواسطة النظام الهجين (الليزر، نفاثة البلازما)

زينب شهيد كاظم ، حيدر يحيى حمود*

قسم الفيزياء، كلية العلوم للبنات، جامعة بغداد، العراق

*البريد الالكتروني للباحث:dr.hayder.y.phy@gmail.com

الخلاصة: يتعامل هذا البحث مع تقييم النشاط المضاد للسرطان لتوليف Ag/Au NPs بواسطة نظام هجين يجمع بين تقنية الليزر والبلازما النفاثة. تمت دراسة تأثير NPs على تثبيط نمو خلايا سرطان الثدي وخط الخلايا الطبيعية. أولاً، تم تحضير الجسيمات النانوية الفضية باستخدام ليزر Nd:YAG بطول موجي 1064 نانومتر، وتردد 6 هرتز، وطاقة 1000 مللي جول، وعدد من النبضات 558. الخطوة الثانية، نأخذ نسبًا مختلفة بين Ag NPs وأملاح الذهب على النحو التالي: (1:9 و 2:8 و 3:7)، على التوالي، وتعرض لنظام نفاث البلازما لمدة 3 دقائق. تم فحص NPs باستخدام حيود الأشعة السينية والتحليل الطيفي للأشعة فوق البنفسجية والمجهر الإلكتروني لمسح الانبعاثات الميدانية (FE-SEM). كان أعلى معدل لتثبيط خلايا سرطان الثدي 66٪ بعد 48 ساعة عندما كان التركيز 100٪ بنسبة 3:7. أما بالنسبة لسمية الخلايا الطبيعية، فإن أعلى سمية كانت 16٪ بعد 24 ساعة عندما كان التركيز 100٪ لمدة 3:7. يمكن أن توفر النتائج المتوقعة ضوءًا جديدًا على فعالية هذه الجسيمات في علاج السرطان وتحفيز الأبحاث المستقبلية في هذا المجال.